



Corrosion behaviour of Ni–Al composite coating in 3.5% NaCl + 0.05 M H₂SO₄ solution

B.I. Onyeachu^{1,2}, E.E. Oguzie², X. Peng^{1*}, C.E. Ogukwe², I. Digbo²

¹State Key Laboratory for Corrosion and Protection, Institute of Metal Research, Chinese Academy of Science, 62 Wencui Road, Shenyang 110016, China

²Electrochemistry and Materials Science Research Laboratory Department of Chemistry, Federal University of Technology Owerri, PMB 1526, Owerri, Nigeria

ABSTRACT

The electrochemical corrosion behaviour of electrodeposited Ni–Al composite coating, containing 1 μm–size Al particles, was studied in 3.5% NaCl + 0.05 M H₂SO₄ solution using electrochemical and surface probe techniques. Open circuit potential measurement revealed that the Al particles shift the Ni corrosion potential to more negative regions. Potentiodynamic polarization characterization showed that the Al particles increase the corrosion rate of the Ni coating by increasing both cathodic and anodic half–reactions. XPS characterization confirmed that the Al corrosion products are highly dissoluble in the 3.5% NaCl + 0.05 M H₂SO₄ solution. This dissolution disturbs the easy linkage of the Ni corrosion product based on SEM characterization.

Keywords: Ni–Al composite; co–electrodeposition; XPS; corrosion rate.

1. INTRODUCTION

Nickel (Ni) is a very important industrial metal due to its strength, resistance to corrosion and can effectively be used for the alloying of many other industrial metals. When micron or sub–micron size particles are deliberately loaded into a conventional Ni electrodeposition bath, the particles are usually entrapped and co–deposited with the growing layer of the Ni coating matrix to form Ni matrix composite coatings. Ni matrix composite coatings usually exhibit better properties like strength [1, 2] and anti–friction [3]. From the perspective of electrochemical corrosion, the resistance of the pure Ni coatings is greatly increased by blocking the surfaces of the Ni grains and reducing the interaction with the corrosion agent by using metal oxides [4–6] as reinforcement particles. This is the mechanism involved with Ni–inert particles composite coatings. Nevertheless, this mechanism can be effectively modified by employing second phase particles of pure metals which will actively partake in the electrochemical reactions and can enrich the Ni corrosion product with highly corrosion–resistant products. Prominent metal particles which can guarantee this modification include Cr and Al. Peng *et al.*, [7] have earlier reported that the general corrosion and pitting corrosion resistance of pure electrodeposited Ni coatings greatly increased in 3.5% NaCl solution when reinforced with Cr nanoparticles, due to enrichment of the Ni corrosion product with Cr–oxides.

Co–electrodeposition of Ni coatings with Al particles will yield Ni–Al composite coatings. At high temperatures, the Al particles can increase the oxidation resistance of pure Ni coatings through the formation of a slow–growing, thermodynamically stable Al₂O₃ scale which also increases the adhesion of the NiO scale with the substrate [8]. Unfortunately, however, the characterization of the effect of the electrochemical corrosion behaviour of Ni–Al coatings has not been given adequate attention. In aqueous solutions, the Al

particles can form the well–known, highly corrosion–resistant Al₂O₃. The growth of a well–developed Al₂O₃ scale, especially in the boundaries of the Ni grains, should assist in the linkage of the Ni corrosion products and lead to the formation of a highly continuous and more protective Ni corrosion product layer, at least in the Al₂O₃–stable pH range of 4–9. Nevertheless, the behaviour of the Al₂O₃ outside this pH range has not been well characterized.

In the present work, we characterize the electrochemical corrosion behaviour of a Ni–Al coating containing, compared with a pure Ni coating, in 3.5% NaCl + 0.05 M H₂SO₄ solution. Our focus is to ascertain the suitability of increasing the electrochemical corrosion resistance of pure Ni coatings with pure metal particles reinforcement, using Al particles as candidate particles.

2. EXPERIMENTAL

2.1. Materials preparation

Pure Ni coupons with dimensions 12 mm x 10 mm x 2 mm were used as substrates for the electrodeposition of the Ni and the Ni–Al composite coatings. The Ni substrates were prepared by mechanically abrading to final 800 mesh size using Si–C grit paper, washed with distilled water, ultrasonically cleaned in acetone to remove adherent particles from the substrate surface, and dried with a mechanical drier. The pure Ni coating was electrodeposited at 2 A/dm² from a Ni sulphate bath containing 150 g/L NiSO₄·6H₂O, 0.1 g/L Sodium Dodecyl Sulphate, 5 g/L NH₄Cl, and 15 g/L H₃BO₃. The Ni–Al composite coating was electrodeposited at 2 A/dm² by loading 200 g of 1 μm–size Al particles into the Ni sulphate bath. A reciprocating perforated plastic stirrer at 175 rpm speed was used as bath agitator. Before the composite deposition, 10 minutes of ultrasonic vibration was performed after loading the Al particles, followed by 40 minutes of mechanical agitation in

order to equilibrate the bath contents. After each deposition, the coatings were rinsed with distilled water, ultrasonically cleaned in acetone, and oven-dried at 105 °C for 2 h. The average Al particles content co-deposited with the Ni coating was 28% by weight.

2.2. Surface feature and corrosion product characterization

A scanning electron microscope (SEM) (FEI-Inspect/OXFORD INSTRUMENTS-X-Max), with EDAX hyphenation (employed for the elemental composition analysis), was employed to characterise the surface morphologies of the Ni and Ni–Al composite coatings in their as-deposited states and after polarization in 3.5% NaCl + 0.05 M H₂SO₄ solution. The corrosion product layer formed on the surface of the polarized Ni–Al composite coating was characterized by x-ray photoelectron spectroscopy (XPS) using XPS-ESCALAB 250 Thermo VG x-ray spectrometer with monochromatic AlK_α (1486.6 eV) radiation source at a pass energy of 1 keV on a sample area of 2 X 2 mm². Spectra peak deconvolution of the Ni 2p_{3/2}, Al 2p_{3/2} and O 1s peaks was performed with the aid of XPSPEAK 4.1 processing software (Chemistry Ltd., CUHK) in the Shirley background after calibrating with the C 1s peak at 284.6 eV.

2.3. Electrochemical Characterization

During the electrochemical characterization, the pure Ni and Ni–Al composite coatings were employed as working electrode samples, prepared by embedding in a mixture of paraffin and rosin to expose a working area of 1cm² for corrosion tests. Saturated calomel electrode (SCE) connected through a Luggin capillary was used as reference electrode and a platinum sheet as counter electrode. The electrochemical methods employed include open circuit potential (E_{OCP}) and potentiodynamic polarization measurements, performed using a PARSTAT 273A Potentiostat/Galvanostat (Princeton Applied Research). The E_{OCP} determination was performed by measuring the potential change with time over a period of 3600 s when the coatings were freely immersed in the 3.5% NaCl + 0.05 M H₂SO₄ solution. Potentiodynamic polarization tests were performed by scanning the coating potentials in the range of –0.25 V/E_{OCP} to +0.25 V/SCE at a scan rate of 0.166 mV/s.

3. RESULTS

Table 1: Polarization parameters for Ni coating and Ni–Al composite in 3.5% NaCl + 0.05 M H₂SO₄ solution

	Ni	Ni-Al
E _{corr} (mV/SCE)	–150	–444
i _{corr} (μA/cm ²)	4.666	6.129

3.3. Surface microstructure of polarized Ni and Ni–Al composite coatings

The SEM surface morphologies of the pure Ni coating and the Ni–Al composite coating after polarization in the 3.5% NaCl +

3.1. Surface microstructure of electrodeposited Ni and Ni–Al composite coatings

The SEM surface morphology of the electrodeposited pure Ni coating is given in Figure 1(a). The image reveals large Ni surface grains; its formation resembles a grain growth mechanism during the reduction of the Ni²⁺ ions on the substrate surface during electrodeposition. The surface morphology of the Ni–Al composite coating with 28wt.% Al particles, Figure 1(b), consists of more refined Ni surface grains with a dense concentration of Al particles clusters in the boundaries of the Ni grains. The particles definitely provide abundant sites on the substrate and promote a nucleation mechanism for the electrodeposition of the Ni grains. Based on EDAX point analysis (not shown here) the Al particles are the spherical particles which appeared darker for those more submerged in the Ni matrix and lighter for those not well embedded.

3.2. Corrosion behaviour of Ni and Ni–Al composite coatings

The plots of change in potential with time for the attainment of E_{OCP} by the Ni and Ni–Al composite coatings during 3600 s in the 3.5% NaCl + 0.05 M H₂SO₄ is provided in Figure 2. It can be seen that a rapid decrease in the potential occurred during the initial 1000 s exposure of the Ni–Al composite coating and, thereafter, the potential remained relatively stable at a more negative value than for the Ni coating. However, the Ni coating maintained relatively stable potential throughout the time. This implies a greater susceptibility to dissolution, and higher rate of the electrochemical processes occurring at the composite surface. The polarization curves for the Ni coating and Ni–Al composite in the 3.5% NaCl + 0.05 M H₂SO₄ solution are given in Figure 3. In Table 1, the corresponding polarization parameters are provided where E_{corr} and i_{corr} represent, respectively, the corrosion potential and corrosion current density, extrapolated from the intersection of the anodic, β_a, and cathodic, β_c, Tafel slopes drawn ±10 mV about the E_{OCP} using Powersuit software. The composite coating exhibited greater i_{corr} value (6.129 μA/cm²) than the Ni coating (4.666 μA/cm²). The Al particles obviously modified the electrochemical corrosion mechanism of the pure Ni coating in the 3.5% NaCl + 0.05 M H₂SO₄, by increasing both cathodic and anodic currents and suppressing an attempt for passivation exhibited by the Ni coating during the anodic scan. Therefore, the Al particles could not guarantee the enrichment of the Ni corrosion layer with a protective Al corrosion product.

0.05 M H₂SO₄ solution are provided in Figure 4. The surface of the Ni coating, Figure 4(a), was characterized by a highly porous layer of corrosion product scale. In Figure 4(b), fine corrosion product layers could be seen forming on the Ni grains, but seriously lacked continuity, clearly due to the detachment

of the surface Al particles. It appears that during the polarization, the Al particles and their corrosion products are highly unstable and lost in the 3.5% NaCl + 0.05 M H₂SO₄ solution.

3.4. Ni–Al composite corrosion product characterization

Figure 5 shows the XPS spectra obtained for the corrosion product layer formed on the surface of the Ni–Al composite coating after polarization in 3.5% NaCl + 0.05 M H₂SO₄ solution. The relevant peaks detected were in the corresponding binding energy ranges: Ni 2p (852–863 eV), Al 2p (72.9 eV–75.4 eV) and O 1s (529–533 eV). The deconvolution of the Ni 2p_{3/2} spectrum gave peaks at 852.7, 854, 856.5 eV which, respectively, correspond to the presence of Ni⁰, NiO and Ni(OH)₂ [9]. The peak at 862.1 eV corresponds to a Ni(OH)₂ satellite peak. The Al 2p_{3/2} spectrum gave peaks at 72.9, 73.8 and 74.9 eV which correspond to the presence of Al⁰ and Al₂O₃ and Al(OH)₃ [10, 11]. The O 1s peaks detected at 530.1, 531.1 eV were attributed to the formation of oxides, hydroxides. Another O 1s peak at 532 eV was, therefore, attributed to adsorbed water molecules. Based on the peak areas, the corrosion product layer contains 48% hydroxides (41% Ni(OH)₂ and 7% Al(OH)₃), and 28% of oxides (20% NiO and 8% Al₂O₃). The composition of the unreacted Ni and Al was very low, relative to the compositions of their corrosion products. Thus, the conversion of the Ni and Al into their corrosion products is very vigorous with the Ni products being more stable than the Al products in the 3.5% NaCl + 0.05 M H₂SO₄ solution.



During the cathodic polarization, the rates of hydrogen evolution and water molecules formation and adsorption increase especially at the numerous defects between the Ni grains and Al particles. During the anodic scan which is related with the dissolution of the Ni and Al species to form their respective oxides, the high concentration of adsorbed water molecules facilitates the conversion of the Ni/Al–oxides into the respective hydroxide species, especially Ni(OH)₂, as revealed by XPS characterization. This weakens the bonding between the Ni grains and Al particles and exposes the Ni–Al composite coating to more aggressive attack by the chloride ions which are electromigrated to the defect sites. The greater loss of the Al products, than the Ni products, could be facilitated by their amphoteric nature, as is well known for Al in the presence of dilute acid solutions. Although the more refined Ni grains in the Ni–Al composite coating could form finer corrosion products around the Ni grains, compared with the pure Ni coating, the effective linkage of this Ni corrosion product layer into a continuous layer is, however, not favoured due to the detachment of the Al particles and the Al corrosion products, as seen in Figure 4. Notwithstanding that the pure Ni coating could not also form a highly continuous corrosion product layer; the degradation of the Ni–Al composite corrosion product layer is more severe than on the pure Ni coating. More so, the loss of the Al products exposes more active surfaces for the dissolution of more Ni grains and Al particles, which eventually cause the higher corrosion current density displayed by the Ni–Al composite coating, relative to the pure Ni coating, in 3.5% NaCl + 0.05 M H₂SO₄ solution. This is, therefore, the reason that the corrosion rate of the Ni–

4. DISCUSSION

The adsorption of water molecules is the primary process which triggers the electrochemical corrosion of pure Ni coating in aqueous electrolyte solution [12]. The electrochemical corrosion behaviour of the Ni coating and the Ni–Al composite can, thus, be explained based on their surface microstructures and the chemistries of the Ni grains and Al particles. It can be reasoned that the more refined Ni surface grains in the composite should cause a higher rate of water molecules adsorption in the high density of Ni grain boundaries saturated with the Al particles. This initiates an abundance of micro electrochemical cells, i.e. active sites on the composite surface. When the Ni–Al composite coating is in contact with the 3.5% NaCl + 0.05 M H₂SO₄ solution, this phenomenon is the reason for the initial decrease in E_{OCP} reaching a stable value more negative than for the pure Ni coating during the open circuit potential measurement. A higher rate of reduction and oxidation reaction would, therefore, occur in these numerous micro electrochemical cells, and cause the higher corrosion current density for the composite coating, as observed during the potentiodynamic polarization. The Al particles reinforcement increases the cathodic and anodic half–reactions occurring on the Ni coating in the 3.5% NaCl + 0.05 M H₂SO₄ solution. Plausible cathodic half–reactions which should occur in the equal–volume mixture of 3.5% NaCl and 0.05 M H₂SO₄ solutions should include the reduction of H⁺ ions and the reduction of oxygen into H₂O (as in an acid medium), as shown below.

Al composite was higher than the pure Ni coating in the 3.5% NaCl + 0.05 M H₂SO₄ solution.

4. CONCLUSION

The reinforcement of electrodeposited Ni coatings with Al particles shifts the Ni corrosion potential to more negative value in 3.5% NaCl + 0.05 M H₂SO₄ solution. It increases the corrosion rate of the Ni coating by increasing both cathodic and anodic reactions. The Al particles can actively participate during the electrochemical corrosion of the Ni coating, but cannot guarantee the enrichment of the Ni corrosion product with the highly resistant Al₂O₃.

Acknowledgements

B.I. Onyeachu is grateful to TWAS, the World Academy of Science and the Chinese Academy of Science (CAS) for the award of a CAS-TWAS Postgraduate Fellowship.

REFERENCES

- Li J, Sun Y, Sun X, Qiao J, Mechanical and corrosion-resistance performance of electrodeposited titania–nickel nanocomposite coatings, *Surface & Coatings Technology* 2005; 192: 331–335
- Zimmerman AF, Palumbo G, Aust KT, Erb U, Mechanical properties of nickel silicon carbide nanocomposites, *Materials Science and Engineering* 2002; A328: 137–146

Shi L, Chufeng S, Gao P, Zhou F, Liu W, Mechanical properties and wear and corrosion resistance of electrodeposited Ni–Co/SiC nanocomposite coating, *Applied Surface Science* 2005; 252: 3591–3599

Szczygiel B, Kolodziej M, Composite Ni/Al₂O₃ coatings and their corrosion resistance, *Electrochimica Acta* 2005; 50: 4188–4195

Feng Q, Li T, Teng H, Zhang X, Zhang Y, Liu C, Jin J, Investigation on the corrosion and oxidation resistance of Ni–Al₂O₃ nano-composite coatings prepared by sediment co-deposition, *Surface & Coatings Technology* 2008; 202: 4137–4144

Hasannejad H, Shahrabi T, Jafarian M, Synthesis and properties of high corrosion resistant Ni–cerium oxide nano-composite coating, *Materials and Corrosion* 2012: 1–10

Peng X, Zhang Y, Zhao J, Wang F, Electrochemical corrosion performance in 3.5% NaCl of the electrodeposited nanocrystalline Ni films with and without dispersions of Cr nanoparticles, *Electrochimica Acta* 2006; 51: 4922–4927

Zhou Y, Peng X, Wang F, Oxidation of a novel electrodeposited Ni–Al nanocomposite film at 1050 °C, *Scripta Materialia* 2004; 50: 1429–1433

Natarajan R, Palaniswamy N, Natesan M, Muralidharan VS, XPS Analysis of Passive Film on Stainless Steel, *The Open Corrosion Journal* 2008; 2: 114-124

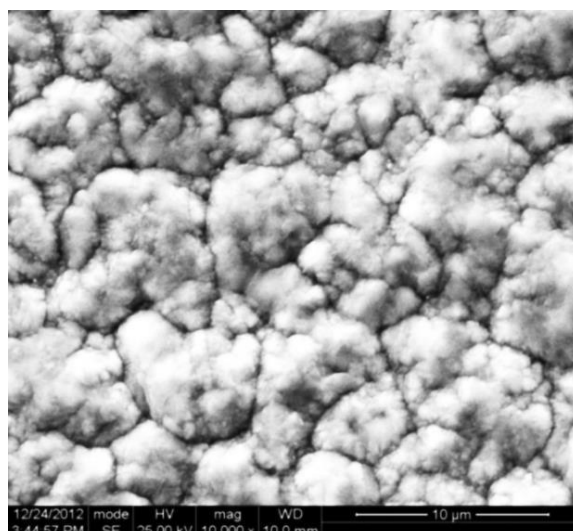
Kontinen P, Kilpi R, Lund PD, Microstructural analysis of selective C/Al₂O₃/Al solar absorber surfaces, *Thin Solid Films* 2003; 425: 24–30

Klopprogge JT, Duong LV, Wood BJ, Frost RL, XPS study of the major minerals in bauxite: gibbsite, bayerite and (pseudo) bohemite. *Journal of Colloid and Interface Science* 2006; 296(2): 572-576

Li-yuan Q, Jian-she L, Qing J, Effect of grain size on corrosion behaviour of electrodeposited bulk nanocrystalline Ni, *Trans Nonferrous Met. Soc. China* 2010: 82–89

Figures

(a)



(b)

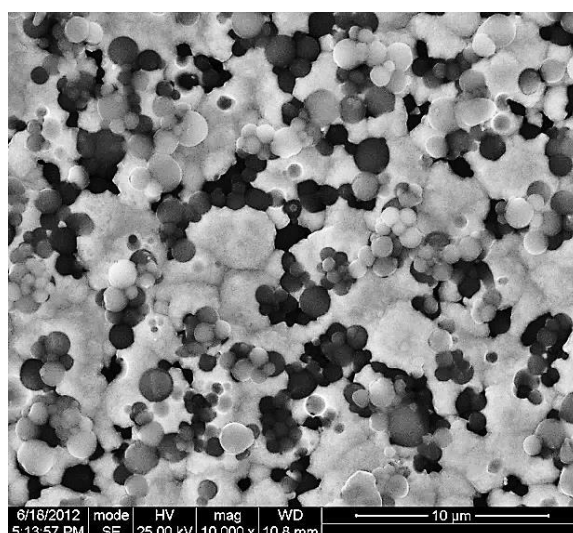


Figure1: SEM surface micrographs of electrodeposited (a) pure Ni coating, and (b) Ni–Al composite containing 28 wt.% Al particles

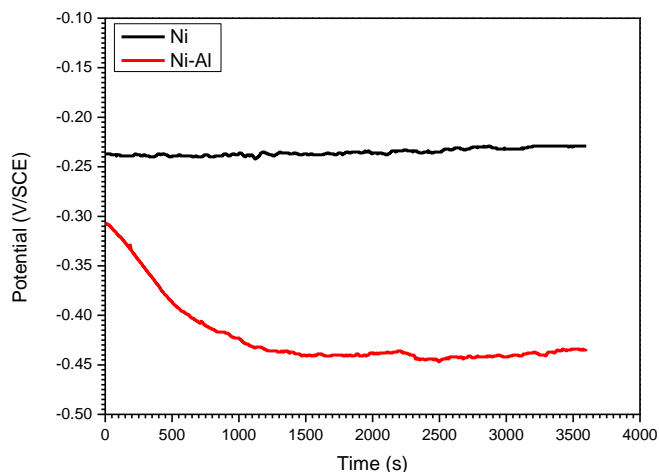


Figure 2: Open Circuit potential for Ni coating and Ni–Al composite coating during 3600 s in 3.5% NaCl + 0.05 M H₂SO₄ solution

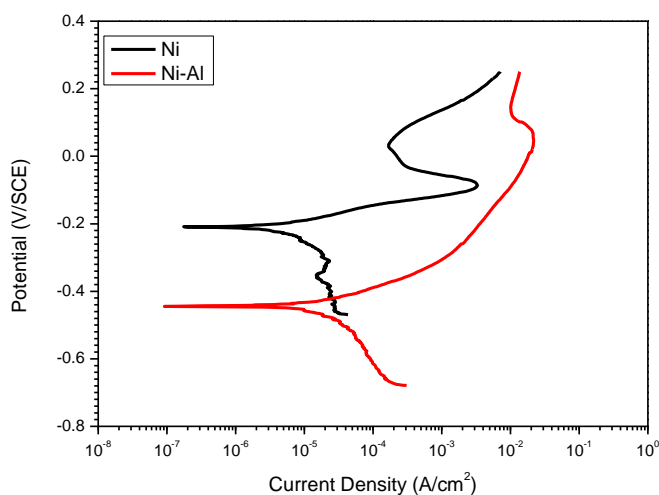
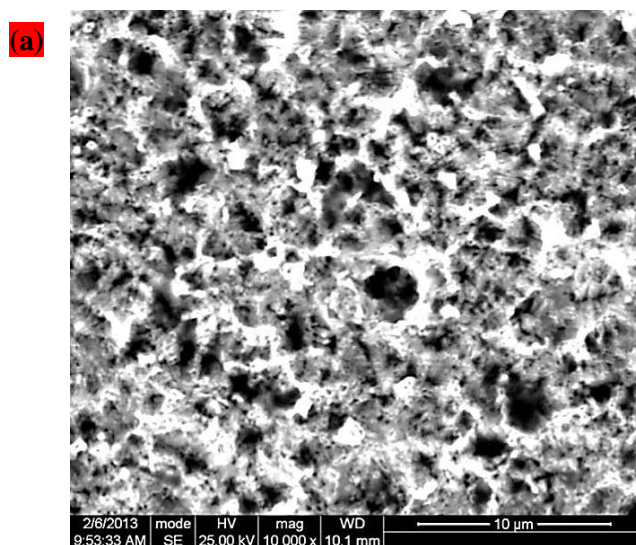


Figure 3: Potentiodynamic polarization curves for Ni coating and Ni–Al composite in 3.5% NaCl + 0.05 M H₂SO₄ solution



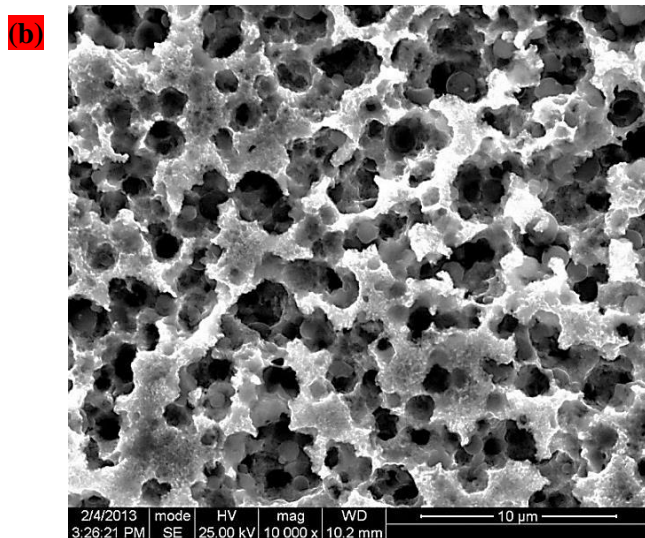


Figure 4: SEM surface micrographs for Ni coating and Ni–Al composite after polarization in 3.5% NaCl + 0.05 M H₂SO₄ solution

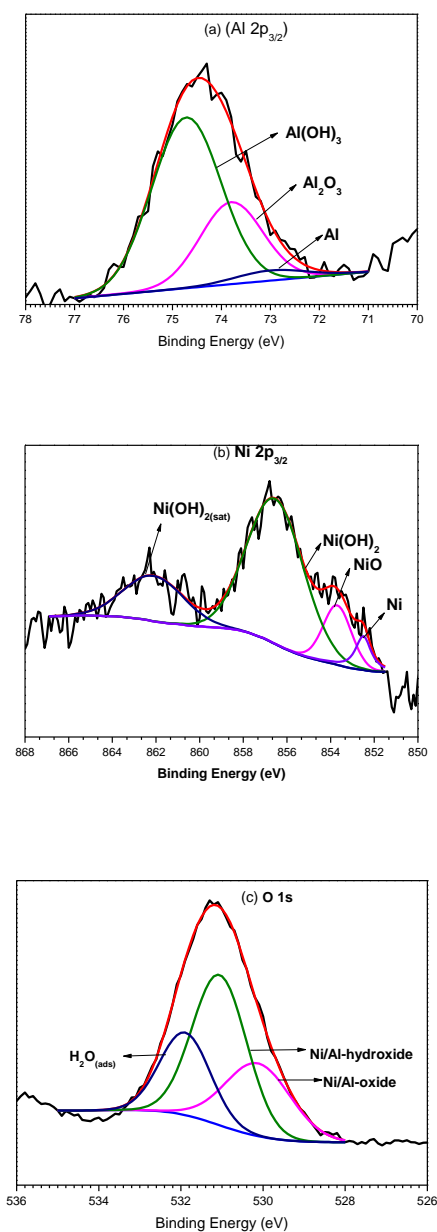


Figure 5: XPS deconvolution of the Ni 2p_{3/2}, Al 2p_{3/2} and O 1s spectra acquired on the surface of Ni–Al composite after polarization in 3.5% NaCl + 0.05 M H₂SO₄ solution